

# Structure–activity relationships of methoctramine-related polyamines as muscarinic antagonist: Effect of replacing the inner polymethylene chain with cyclic moieties

Vincenzo Tumiatto,<sup>a,\*</sup> Anna Minarini,<sup>a</sup> Andrea Milelli,<sup>a</sup> Michela Rosini,<sup>a</sup>  
Michela Buccioni,<sup>b</sup> Gabriella Marucci,<sup>b</sup> Carla Ghelardini,<sup>c</sup>  
Cristina Bellucci<sup>d</sup> and Carlo Melchiorre<sup>a</sup>

<sup>a</sup>*Dipartimento di Scienze Farmaceutiche, Università di Bologna, Via Belmeloro 6, 40126 Bologna, Italy*

<sup>b</sup>*Dipartimento di Scienze Chimiche, Università di Camerino, Via S. Agostino 1, 62032 Camerino, Italy*

<sup>c</sup>*Dipartimento di Farmacologia Preclinica e Clinica, Università di Firenze, Viale Pieraccini 6, 50139 Firenze, Italy*

<sup>d</sup>*Dipartimento di Scienze Farmaceutiche, Università di Firenze, Via Ugo Schiff 6, 50026 Sesto Fiorentino, Firenze, Italy*

Received 28 November 2006; revised 8 January 2007; accepted 17 January 2007

Available online 19 January 2007

**Abstract**—The aim of the present paper was to investigate the role of the octamethylene spacer of methoctramine (**1**) on the biological profile. Thus, this spacer was incorporated into a dianiline or dipiperidine moiety to determine whether flexibility and the basicity of the inner nitrogen atoms are important determinants of potency with respect to muscarinic receptors. The most potent compound was **4**, which displayed, in the functional assays, a comparable potency at muscarinic M<sub>2</sub> receptors with respect to **1**, and, in the binding assays, a loss of potency and selectivity toward muscarinic M<sub>1</sub> and M<sub>3</sub> receptor subtypes. Both compounds were endowed with antinociceptive activity. Furthermore, in microdialysis tests in rat parietal cortex, they enhanced acetylcholine release, most likely by antagonizing presynaptic muscarinic receptor subtypes.

© 2007 Elsevier Ltd. All rights reserved.

## 1. Introduction

Muscarinic receptors are widely distributed in the central and peripheral nervous system. They are mainly located on the autonomic effector cells of postganglionic parasympathetic nerves and also in the brain, ganglia, and blood vessels with cholinergic innervation. They play an important role in regulating the activity of several vital functions such as control of movement, cognition, smooth muscle tone, and glandular secretion.<sup>1,2</sup> To date, molecular cloning techniques have led to the discovery and identification of five muscarinic receptor subtypes, namely, M<sub>1</sub>–M<sub>5</sub>. Only four (M<sub>1</sub>–M<sub>4</sub>) have been pharmacologically characterized, however, and little information is available about the nature and the cellular location of the M<sub>5</sub> subtype.<sup>3–6</sup> The five muscarinic receptor subtypes belong to the superfamily of G-protein-coupled receptors and include seven hydrophobic

regions, which form  $\alpha$ -helical transmembrane domains connected by alternating intracellular and extracellular loops.<sup>7</sup> Fundamental information has been gained by using selective chemically synthesized ligands<sup>8,9</sup> as well as transgenic mice lacking genes encoding each of the five muscarinic receptor subtypes<sup>10–12</sup> and muscarinic toxins from snake venoms.<sup>13–16</sup> Despite these efforts, very few selective ligands are available to characterize muscarinic receptors.

Attempts to develop selective compounds have been hampered by the high degree of homology between receptor subtypes within the binding region of acetylcholine (ACh) and other small molecules.<sup>17,18</sup>

Nonselective ligands exhibit many undesirable side effects that limit their clinical usefulness. For this reason, the number of muscarinic receptor agonists and antagonists that have been introduced in therapy is modest. In particular, muscarinic receptor antagonists are used therapeutically for the treatment of smooth muscle disorders including urinary incontinence, irritable

**Keywords:** Methoctramine; Polyamines; Muscarinic antagonists; Pain.

\* Corresponding author. Tel.: +39 0512099709; fax: +39 0512099734;  
e-mail: [vincenzo.tumiatto@unibo.it](mailto:vincenzo.tumiatto@unibo.it)

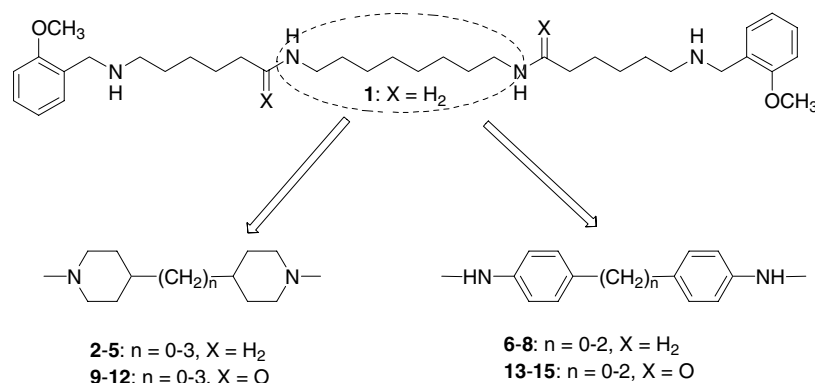


**Figure 1.** Chemical structure of methoctramine (**1**). The design strategy for the development of **2–15** is also shown.

bowel syndrome, and chronic obstructive pulmonary disease.<sup>8,19–22</sup>

Nevertheless, research into newer and more selective muscarinic receptor ligands is still ongoing and active. For instance, selective muscarinic M<sub>1</sub> receptor agonists and muscarinic M<sub>2</sub> receptor antagonists, by interacting directly with post-synaptic muscarinic receptors or by antagonizing muscarinic M<sub>2</sub> autoreceptors, respectively, may be useful in enhancing cognitive function in individuals affected by Alzheimer's disease,<sup>2,23–26</sup> as well as for the treatment of moderate to severe acute pain. To this end, various strategies to induce analgesia of cholinergic type have been reported, through direct stimulation of postsynaptic muscarinic M<sub>1</sub> receptor or inhibition of presynaptic muscarinic M<sub>2</sub> receptors. Recent evidence indicates the involvement of these latter receptor subtypes in pain regulation by modulating the endogenous ACh release.<sup>25,27–30</sup>

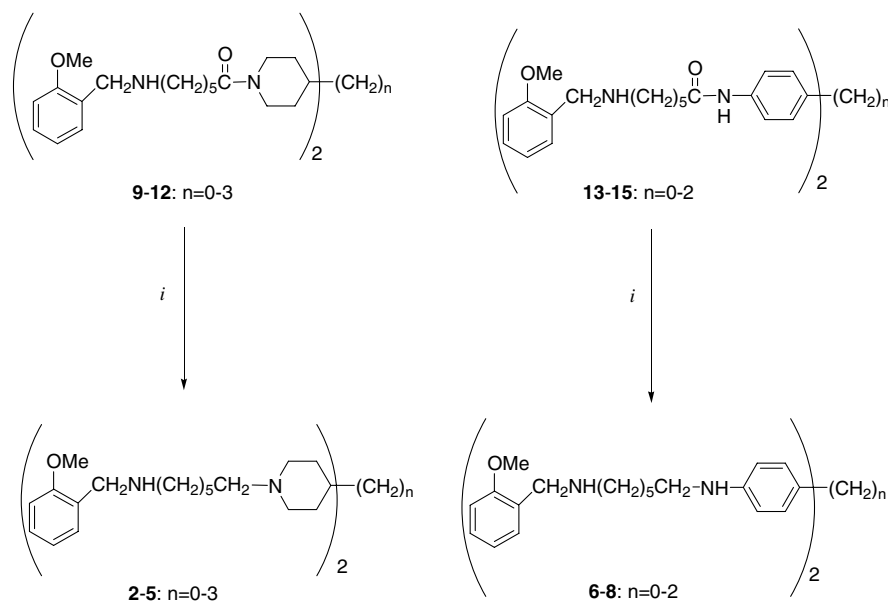
For a long time, our group has been involved in the research of selective muscarinic receptor ligands by applying the 'universal template approach'. According to this approach, we hypothesized that a polymethylene tetraamine backbone may represent a universal template on which suitable pharmacophores can be inserted to achieve selectivity for any given receptor or enzymatic system.<sup>31–33</sup> The application of this concept has allowed us, for instance, to design polyamines displaying high affinity and selectivity for muscarinic M<sub>2</sub> receptors, which we achieved by introducing appropriate pharmacophores on the polyamine backbone of methoctramine (**1**),<sup>34</sup> a well-known selective muscarinic M<sub>2</sub> receptor antagonist.<sup>33,35</sup> The same concept, applied on different targets such as acetylcholinesterase (AChE), led to the discovery of new polyamines able to inhibit AChE.<sup>36–38</sup> The polyamine backbone, thanks to its flexibility, may assume many low-energy conformations in an aqueous environment. To reduce the conformational freedom of the polymethylene chain and to determine whether flexibility is an important determinant of potency with respect to muscarinic receptors, we designed a series of **1**-related compounds in which the inner octamethylene chain of **1** was incorporated partially or totally into a more constrained moiety as shown in Figure 1. The flexibility reduction approach on **1**-structure was

already successfully applied to give PIP (1,1''-(1,8-octanediyl)bis[1'-[(2-methoxyphenyl)methyl]-4,4'-bipiperidine] and PIPAM (1,1''-(1,8-dioxo-1,8-octanediyl) bis[1'-[(2-methoxyphenyl)methyl]-4,4'-bipiperidine), endowed with an original and not entirely characterized biological profile,<sup>39,40</sup> and new selective nicotinic receptor polyamine-based ligands.<sup>41</sup>

In the present work, the inner diamino-octane spacer of **1** was replaced by the less flexible dipiperidine or dianiline moiety, affording **2–8** (Fig. 1). We included in this study diamine-diamides **9–15** because we had already verified that the inner amine functions can be transformed into the corresponding amide groups without affecting dramatically the affinity toward muscarinic receptors.<sup>32</sup> All the synthesized compounds were tested at peripheral muscarinic M<sub>2</sub> and M<sub>3</sub> receptor subtypes as well as at the muscarinic receptor located in the rabbit vas deferens, a putative muscarinic M<sub>4</sub> receptor subtype.<sup>42</sup> Furthermore, the biological profile of the most potent muscarinic receptor antagonist of the series, **4**, was investigated further by performing binding assays in CHO cells expressing human muscarinic receptors. The promising biological profile of **4** prompted us to evaluate its behavior in other assays in which the cholinergic system is involved. For this reason, we carried out antinociceptive assays for both derivatives **4** and **1**. In addition, we measured the ability of **4** to inhibit AChE, because an increase of ACh in synaptic cleft would contribute to the antinociceptive activity. This assay was also carried out on **11**, since this compound is related to some diamine-diamides endowed with this activity.<sup>36</sup> Finally, we verified whether **4** is able to improve the ACh release in rat frontal cortex by microdialysis experiments.

## 2. Chemistry

All the compounds were synthesized by standard procedures (Scheme 1) and were characterized by IR, <sup>1</sup>H NMR, mass spectra, and elemental analysis. The synthesis of the starting diamine-diamides **9–15** was performed following a previously reported procedure.<sup>43</sup> Tetraamines **2–8** were prepared by reduction of **9–15** with BACH-EI in dry diglyme.



Scheme 1. Reagents: (i) BACH-EI, diglyme.

### 3. Biology

#### 3.1. Functional studies

The pharmacological profile at functional muscarinic receptor subtypes of **2-15** was assessed in vitro on stimulated guinea pig left atria ( $M_2$ -subtype),<sup>44</sup> ileum ( $M_3$ -subtype),<sup>45</sup> and rabbit vas deferens.<sup>46</sup> The results were expressed in terms of  $pK_b$ .<sup>47</sup> For a long time, the contraction of rabbit vas deferens was referred to as an effect mediated by  $M_1$ -receptor subtypes,<sup>46,48</sup> even though some more recent studies attribute the same effect to an  $M_4$ -activation.<sup>42</sup> For this reason, in the present paper, the rabbit vas deferens will be considered an  $M_4$ -putative muscarinic receptor subtype.

#### 3.2. Binding experiments

Muscarinic receptor affinity was evaluated in CHO cells expressing the five human muscarinic receptor subtypes (hm1–hm5).

#### 3.3. Antinociceptive test

The antinociceptive activity was established by the mouse hot plate test as described by O'Callaghan and Holtzman.<sup>49</sup>

#### 3.4. Acetylcholine release

To determine the increase of ACh in the synaptic cleft, we carried out some microdialysis experiments in rat parietal cortex as described by Giovannini et al.<sup>50</sup> The increase of ACh level was determined by HPLC injection of the perfusate, collected using the microdialyzed technique.

#### 3.5. AChE and butyrylcholinesterase (BChE) inhibition studies

The inhibitory potency of **4** and **11** of recombinant human AChE and BChE was evaluated by studying the hydrolysis of acetylthiocholine following the method of Ellman et al.<sup>51</sup> The inhibitory potency was expressed as  $pIC_{50}$  value, which represents the negative logarithm of the concentration of inhibitor required to decrease enzyme activity by 50%. To allow comparison of the results, **1** was used as the reference compound.

In all the above experiments, to allow comparison of the results, **1** was used as the reference compound.

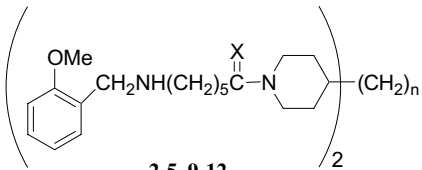
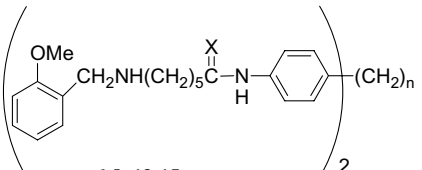
### 4. Results and discussion

The antagonistic potency, expressed as  $pK_b$  values, of compounds **2-15** at peripheral muscarinic  $M_2$  and  $M_3$ , and putative  $M_4$  receptors is shown in Table 1.

Furthermore, to better elucidate the pharmacological profile of the most potent muscarinic receptor antagonist, **4**, binding assays were performed on human cloned muscarinic receptor subtypes (Table 2). In addition, the inhibitory potency, expressed as  $pIC_{50}$  values (Table 1), of AChE and BChE of **4** and its precursor **11** was determined on human recombinant AChE and BChE (Table 3). The antinociceptive activities of **1** and **4** were determined by performing hot plate tests (Tables 3 and 4). To verify the nature of the antinociceptive effect, the ACh release induced by **4** was evaluated as well (Fig. 2). In all these assays, compound **1** was used as reference compound.

An analysis of the results reveals that, in the functional assays (Table 1), the most active derivatives **2-5** belong

**Table 1.** Biological activities of derivatives **2–15**

			
2-5, 9-12		6-8, 13-15	

Compound	X	n	pK <sub>b</sub> <sup>a</sup>			pIC <sub>50</sub> <sup>b</sup> (AChE)	pIC <sub>50</sub> <sup>b</sup> (BChE)
			M <sub>2</sub>	M <sub>3</sub>	M <sub>4</sub>		
1			7.82 ± 0.02	6.32 ± 0.07	6.45 ± 0.09	5.27 ± 0.03 <sup>d</sup>	6.01 ± 0.02 <sup>d</sup>
2	H <sub>2</sub>	0	7.12 ± 0.01	6.08 ± 0.24	6.13 ± 0.06		
3	H <sub>2</sub>	1	7.16 ± 0.06	5.82 ± 0.10	5.39 ± 0.01		
4	H <sub>2</sub>	2	7.98 ± 0.05	6.58 ± 0.05	5.56 ± 0.07	5.89 ± 0.02	4.98 ± 0.05
5	H <sub>2</sub>	3	7.52 ± 0.12	6.37 ± 0.16	5.64 ± 0.15		
6	H <sub>2</sub>	0	<5	— <sup>c</sup>	<5		
7	H <sub>2</sub>	1	<5	5.35 ± 0.12	<5		
8	H <sub>2</sub>	2	<5	— <sup>c</sup>	<5.52		
9	O	0	6.50 ± 0.28	5.62 ± 0.16	6.00 ± 0.10		
10	O	1	6.29 ± 0.10	5.48 ± 0.11	5.37 ± 0.13		
11	O	2	5.91 ± 0.11	5.14 ± 0.10	6.09 ± 0.19	6.87 ± 0.03	4.73 ± 0.03
12	O	3	5.11 ± 0.07	5.09 ± 0.06	<5		
13	O	0	5.31 ± 0.24	— <sup>c</sup>	5.21 ± 0.09		
14	O	1	5.47 ± 0.07	5.32 ± 0.13	<5		
15	O	2	<5	<5	<5		

Antagonist affinities, expressed as pK<sub>b</sub> values, at muscarinic receptors of the isolated guinea pig atrium (M<sub>2</sub>) and ileum (M<sub>3</sub>), and rabbit vas deferens (M<sub>4</sub>), and AChE and BChE inhibiting potency, expressed as pIC<sub>50</sub> values, of **2–15** in comparison to **1**.

All data are presented as means ± SE of 4 or 5 experiments.

<sup>a</sup> The antagonist potency was expressed by pK<sub>b</sub> values<sup>55</sup> calculated at one or two concentrations.

<sup>b</sup> AChE and BChE were from human erythrocytes and human serum, respectively. pIC<sub>50</sub> values represent the negative logarithm of the concentration of inhibitor required to decrease enzyme activity by 50% and are means of two independent measurements, each performed in triplicate.

<sup>c</sup> At 3 μM concentration, a tissue desensitization was observed.

<sup>d</sup> Data from Ref. 38.

**Table 2.** Affinity estimates, expressed as pK<sub>i</sub> values, of **1** and **4** for the five human muscarinic receptor subtypes expressed in CHO cells

Compound	pK <sub>i</sub> <sup>a</sup>				
	M <sub>1</sub>	M <sub>2</sub>	M <sub>3</sub>	M <sub>4</sub>	M <sub>5</sub>
<b>1</b>	7.08 ± 0.06	8.62 ± 0.12	6.28 ± 0.04	6.97 ± 0.10	6.26 ± 0.12
<b>4</b>	7.70 ± 0.15	8.22 ± 0.16	6.67 ± 0.10	7.39 ± 0.11	6.77 ± 0.12

<sup>a</sup> The affinity estimates (pK<sub>i</sub>) were derived from the IC<sub>50</sub> values using the Cheng-Prusoff equation and are means ± SEM of at least three independent experiments. IC<sub>50</sub> values were derived from displacement of [<sup>3</sup>H]-NMS.

**Table 3.** Effects of **1** in the mouse hot plate test<sup>a</sup>

Treatment (icv)	Licking latency in mice (s)				
	Before treatment	After treatment			
		15 min	30 min	45 min	60 min
SALINE	14.2 ± 1.0	15.0 ± 1.3	14.9 ± 1.7	13.8 ± 1.1	14.1 ± 1.5
<b>1</b> (0.005 μg)	14.6 ± 1.2	20.2 ± 1.6 <sup>b</sup>	18.4 ± 2.3	18.3 ± 1.6	16.6 ± 1.5
<b>1</b> (0.01 μg)	13.8 ± 0.9	23.4 ± 1.7 <sup>b</sup>	22.5 ± 2.0 <sup>b</sup>	19.3 ± 1.9	17.2 ± 1.3
<b>1</b> (0.05 μg)	14.5 ± 0.7	24.1 ± 2.6 <sup>b</sup>	23.9 ± 2.5 <sup>b</sup>	18.7 ± 2.1	14.4 ± 1.9
<b>1</b> (1.0 μg)	15.8 ± 1.1	20.6 ± 1.8 <sup>b</sup>	21.3 ± 1.7 <sup>b</sup>	17.5 ± 1.8	15.5 ± 1.2
Naloxone + <b>1</b> (0.01 μg) <sup>c</sup>	15.1 ± 1.0	25.4 ± 1.7 <sup>b</sup>	23.6 ± 2.1 <sup>b</sup>	16.9 ± 1.6	14.8 ± 1.8
Atropine + <b>1</b> (0.01 μg) <sup>c</sup>	14.9 ± 1.7	15.9 ± 1.8	16.5 ± 2.0	15.3 ± 1.5	16.7 ± 1.6

<sup>a</sup> Mice treated with **1** at the dose of 3.0 μg icv were extremely excited and devoid of motor coordination.

<sup>b</sup> P < 0.01 in comparison with saline-controls. Each value represents the mean of at least 17 mice.

<sup>c</sup> Naloxone 1 mg/kg ip and atropine 5 mg/kg ip were injected 10 min before **1**. These two antagonists, when administered alone, did not modify pain threshold.

to the dipiperidine series, while the dianiline derivatives **6–8** and **13–15**, and the dipiperidino-diamide derivatives **9–12** displayed weak antagonistic activity towards the

three investigated muscarinic receptor subtypes. In particular, derivative **4** was almost as active as the reference compound **1** at the muscarinic M<sub>2</sub> receptor with a

**Table 4.** Effects of **4** in the mouse hot plate test<sup>a</sup>

Treatment (icv)	Licking latency in mice (s)				
	Before treatment	After treatment			
		15 min	30 min	45 min	60 min
SALINE	15.6 ± 1.0	17.2 ± 1.6	14.6 ± 1.9	16.7 ± 1.5	18.0 ± 1.9
<b>4</b> (0.01 µg)	14.4 ± 1.1	15.9 ± 1.8	17.1 ± 2.1	18.6 ± 2.0	14.2 ± 1.8
<b>4</b> (0.03 µg)	15.2 ± 1.4	18.6 ± 1.3	19.4 ± 2.2	18.3 ± 2.1	16.1 ± 1.6
<b>4</b> (0.1 µg)	13.9 ± 0.8	24.7 ± 1.3 <sup>b</sup>	24.5 ± 1.4 <sup>b</sup>	22.1 ± 1.3 <sup>b</sup>	18.6 ± 1.5
<b>4</b> (0.3 µg)	14.3 ± 1.1	23.8 ± 1.5 <sup>b</sup>	25.0 ± 2.5 <sup>b</sup>	20.1 ± 1.8 <sup>b</sup>	15.7 ± 1.8
<b>4</b> (1.0 µg)	16.0 ± 1.2	19.3 ± 1.8	21.3 ± 2.2 <sup>b</sup>	18.5 ± 2.1	19.5 ± 1.6
<b>4</b> (10 µg)	16.1 ± 1.3	13.3 ± 1.5	15.6 ± 1.7	17.7 ± 1.8	18.3 ± 2.1
Naloxone + <b>4</b> (0.1 µg) <sup>c</sup>	14.9 ± 1.1	26.2 ± 2.0 <sup>b</sup>	25.3 ± 2.2 <sup>b</sup>	19.9 ± 1.7	17.4 ± 2.4
Atropine + <b>4</b> (0.1 µg) <sup>c</sup>	15.5 ± 1.8	17.4 ± 1.6	17.1 ± 1.9	14.5 ± 1.5	13.2 ± 1.5

<sup>a</sup> Mice treated with **4** at the dose of 50 µg icv were extremely excited and devoid of motor coordination.

<sup>b</sup>  $P < 0.01$  in comparison with saline-controls. Each value represents the mean of at least 14 mice (two experiments).

<sup>c</sup> Naloxone 1 mg/kg ip and atropine 5 mg/kg ip were injected 10 min before **4**. These two antagonists, when administered alone, did not modify pain threshold.

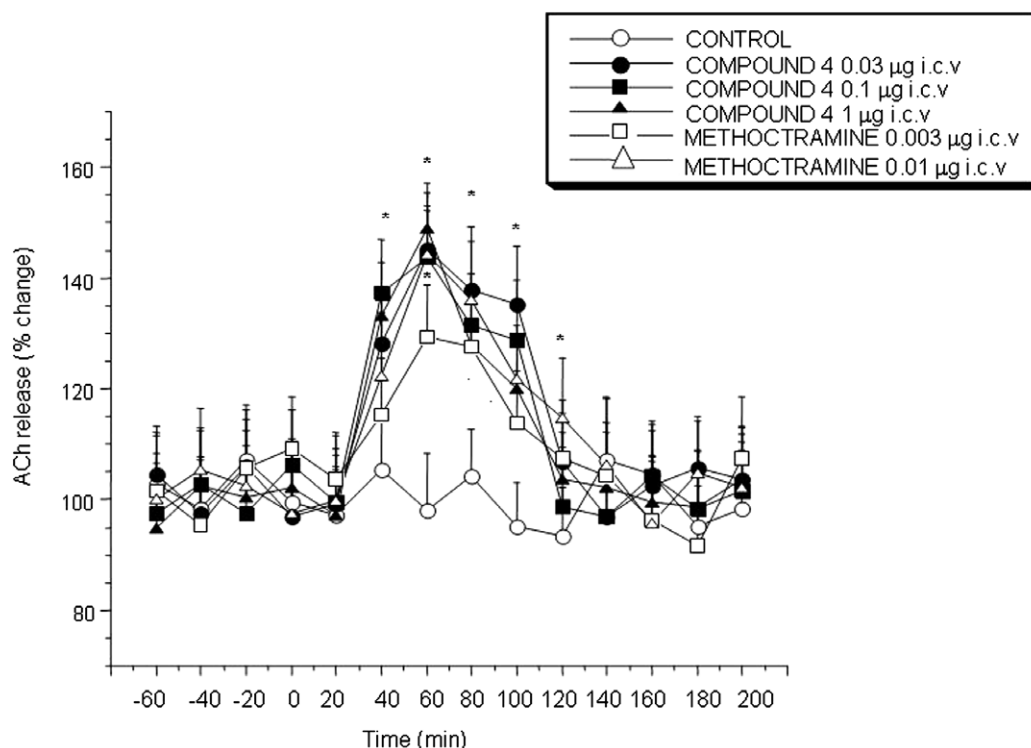


**Figure 2.** Dose–response curve for compound **4** and the reference compound **1**. The two compounds were injected icv at time 0. All values are expressed as changes over basal output. Vertical lines give SEM. Each point represents the mean of three experiments. \* $p < 0.05$ .

similar selectivity profile. The dianilines **6–8** and **13–15** were weak muscarinic  $M_2$  receptor antagonists, outlining the request of four aliphatic basic nitrogen atoms for an optimal interaction with this receptor subtypes.

The biological profile of **4** was also assessed by binding assays on human cloned muscarinic receptors through comparison with **1** (Table 2). Derivative **4**, although displaying a lower affinity for muscarinic  $M_2$  receptors in comparison with the functional tests, showed a selectivity profile similar to that of **1** ( $M_2 > M_1 > M_4 > M_3 = M_5$ ). Interestingly, derivative **4** inhibited AChE with higher potency than **1** (Table 1). As expected, the

corresponding diamino-diamide derivative **11** showed a greater AChE inhibitory potency than **4**, as previously shown for related diamino-diamides when compared with the corresponding tetramines.<sup>52</sup>

As outlined above, muscarinic  $M_2$  antagonists may be useful in the treatment of pain by interacting with presynaptic receptors and hence facilitating ACh release. Thus, mouse hot plate tests were performed to determine the antinociceptive action of the most potent antagonist **4**, when compared with the reference compound **1** (Tables 3 and 4). An analysis of the results shows that **1** and **4** are effectively endowed with



antinociceptive activity and **1** is more potent than **4**. In particular, **1** displayed its antinociceptive effects after 15 min at concentrations as low as 0.005  $\mu\text{g}$ , while **4** was effective only at a concentration of 0.03  $\mu\text{g}$ . In addition, **1** reached the maximum effect at 0.05  $\mu\text{g}$  concentration, while **4** showed the same effect at 0.3  $\mu\text{g}$  concentration. These effects were not reverted by naloxone, indicating a non-opioid effect. They were reverted by administration of atropine, however, indicating a muscarinic effect. It is worth noting that, in the hot plate tests, fairly similar antinociceptive effects were obtained by oral administration of the structurally similar 9-*N,N*-diethyl derivative,<sup>37</sup> previously reported as a potent AChE inhibitor, confirming the cholinergic nature of the antinociceptive action (Ghelardini et al. unpublished results). Consequently, we measured the inhibition of AChE and the ACh release in the synaptic cleft by microdialysis in rat parietal cortex (Fig. 2). Compound **4** enhanced ACh release. The maximum effect was reached 60 min after administration and persisted for up to 100 min after administration. These data confirmed the effective increase of ACh release caused by **4**, which could act by blocking the muscarinic  $M_2$  presynaptic autoreceptors. Furthermore, the poor selectivity showed by **4** could explain the loss of antinociceptive activity at higher doses caused by the postsynaptic muscarinic receptor blockade.

## 5. Conclusions

The present investigation has demonstrated that the replacement of the inner linear polymethylene chain of **1** with a bicyclic moiety preserved the muscarinic activity observed for the lead compound **1**. The most active compound of this new series of polyamines was dipiperidine **4**, whose distance between the two inner nitrogen atoms is similar to the distance from the two basic inner nitrogen atoms of **1**. In the mouse hot plate tests, the behavior of **1** and **4** was quite similar, although **4** was less potent. The AChE inhibitory activity showed by **4** may contribute to the increase of ACh in the synaptic cleft. Finally, ACh release assays demonstrated the efficacy of **4** in enhancing the ACh release in rat parietal cortex caused by muscarinic  $M_2$  presynaptic autoreceptor blockade.

## 6. Experimental

### 6.1. Chemistry

Melting points were taken in glass capillary tubes on a Buechi SMP-20 apparatus and are uncorrected. Electron impact (EI) mass and direct infusion ESI-MS spectra were recorded on VG 7070E and Waters ZQ 4000 apparatus, respectively.  $^1\text{H}$  NMR spectra were recorded on Varian VXR 300 instrument. Chemical shifts are reported in parts per million (ppm) relative to tetramethylsilane (TMS), and spin multiplicities are given as s (singlet), br s (broad singlet), d (doublet), q (quartet), t (triplet), or m (multiplet). The elemental compositions of the compounds agreed to within  $\pm 0.4\%$  of the

calculated value. When the elemental analysis is not included, crude compounds were used in the next step without further purification. Chromatographic separations were performed on silica gel columns by flash (Kieselgel 40, 0.040–0.063 mm; Merck) or gravity column (Kieselgel 60, 0.063–0.200 mm; Merck) chromatography. Reactions were followed by thin-layer chromatography (TLC) on Merck (0.25 mm) glass-packed precoated silica gel plates (60 F254) that were visualized in an iodine chamber. The term ‘dried’ refers to the use of anhydrous sodium sulfate. Compounds were named following IUPAC rules as applied by Beilstein-Institut AutoNom (version 2.1), a PC integrated software package for systematic names in organic chemistry.

**6.2. General procedure for the synthesis of 6,6'-(4,4'-bipiperidine-1,1'-diyl)bis(*N*-(2-methoxybenzyl)hexan-1-amine) (2), 6,6'-(4,4'-methylenebis(piperidine-4,1-diyl))bis(*N*-(2-methoxybenzyl)hexan-1-amine) (3), 6,6'-(4,4'-(ethane-1,2-diyl)bis(piperidine-4,1-diyl))bis(*N*-(2-methoxybenzyl)hexan-1-amine) (4), 6,6'-(4,4'-(propane-1,3-diyl)bis(piperidine-4,1-diyl))bis(*N*-(2-methoxybenzyl)hexan-1-amine) (5), *N*1,*N*1'-(biphenyl-4,4'-diyl)bis(*N*6-(2-methoxybenzyl)hexane-1,6-diamine) (6), *N*1,*N*1'-(4,4'-methylenebis(4,1-phenylene))bis(*N*6-(2-methoxybenzyl)hexane-1,6-diamine) (7), and *N*1,*N*1'-(4,4'-(ethane-1,2-diyl)bis(4,1-phenylene))bis(*N*6-(2-methoxybenzyl)hexane-1,6-diamine) (8)**

A solution of 2 M BACH-EI<sup>TM</sup> in tetrahydrofuran (4 mL) was added dropwise at room temperature to a solution of **9–15**<sup>36</sup> (2 mmol) in dry diglyme (10 mL) under a stream of dry nitrogen. When the addition was completed, the reaction mixture was heated at reflux temperature for 5 h. After cooling at room temperature, excess borane was destroyed by cautious dropwise addition of water (4 mL) and 6 N HCl (4 mL). The resulting mixture was then heated at reflux temperature for 1 h. After solvent evaporation, the crude product was washed with ethyl ether (3  $\times$  15 mL), then the mixture was made basic with aqueous 35% NaOH and extracted with  $\text{CHCl}_3$  (4  $\times$  50 mL). Removal of the dried solvent gave a residue that was purified by gravity column chromatography. Elution with the appropriate solvent gave compounds **2–8** as free bases, that were converted into the tetraoxalates **2–5** and dioxalates **6–8**, and recrystallized from IprOH/MeOH.

**Compound 2.** Eluting solvent, from  $\text{CH}_2\text{Cl}_2/\text{EtOAc}/\text{MeOH}/\text{toluene}/\text{aqueous } 28\% \text{ ammonia}$  (5:2:1:2:0.15) to  $\text{CH}_2\text{Cl}_2/\text{EtOAc}/\text{MeOH}/\text{toluene}/\text{aqueous } 28\% \text{ ammonia}$  (4.5:2:1.5:2:0.2); yellow pale oil; 33% yield;  $^1\text{H}$  NMR( $\text{CDCl}_3$ , free base)  $\delta$  1.30–1.50 (m, 24H+2H exchangeable with  $\text{D}_2\text{O}$ ), 1.64 (d, 2H,  $J = 7$  Hz), 1.82 (t, 4H,  $J = 5.8$  Hz), 2.27 (t, 4H,  $J = 8$  Hz), 2.58 (t, 4H,  $J = 7.2$  Hz), 2.94 (d, 4H,  $J = 11$  Hz), 3.78 (s, 4H), 3.83 (s, 6H), 6.83–7.23 (m, 8H); EI-MS  $m/z$  608 ( $\text{M}^+$ ); mp (tetraoxalate salt) 138–139  $^\circ\text{C}$ . Anal. ( $\text{C}_{46}\text{H}_{70}\text{N}_4\text{O}_{18} \cdot 2\text{H}_2\text{O}$ ) C, H, N.

**Compound 3.** Eluting solvent,  $\text{MeOH}/\text{CH}_2\text{Cl}_2/\text{toluene}/\text{aqueous } 28\% \text{ ammonia}$  (4.5:3:1:0.2); colorless oil; 59%

yield;  $^1\text{H}$  NMR ( $\text{CDCl}_3$ , free base)  $\delta$  1.62–1.70 (m, 28H), 1.86 (t, 4H,  $J = 5.8$  Hz), 2.08 (br s, 2H exch), 2.27 (t, 4H,  $J = 8$  Hz), 2.59 (t, 4H,  $J = 7.2$  Hz), 2.92 (d, 4H,  $J = 11$  Hz), 3.79 (s, 4H), 3.84 (s, 6H), 6.84–6.95 (m, 4H), 7.21–7.30 (m, 4H); EI-MS  $m/z$  621 ( $\text{M}^+$ ); mp (tetraoxalate salt) 155–156 °C. Anal. ( $\text{C}_{47}\text{H}_{72}\text{N}_4\text{O}_{18}$ ) C, H, N.

**Compound 4.** Eluting solvent,  $\text{MeOH}/\text{CH}_2\text{Cl}_2/\text{toluene}/\text{aqueous } 28\% \text{ ammonia}$  (4.5:1.5:3:0.2); colorless amorphous solid (free base); mp 55–57 °C; 51% yield;  $^1\text{H}$  NMR ( $\text{CDCl}_3$ , free base)  $\delta$  1.24–1.75 (m, 30H), 1.91 (t, 4H,  $J = 5.8$  Hz), 2.04 (s, 2H), 2.34 (t, 4H,  $J = 8$  Hz), 2.60 (t, 4H,  $J = 7$  Hz), 2.96 (d, 4H,  $J = 11$  Hz), 3.81 (s, 4H), 3.86 (s, 6H), 6.87–6.93 (m, 4H), 7.23–7.29 (m, 4H); EI-MS  $m/z$  636 ( $\text{M}^+$ ); mp (tetraoxalate salt) 197–200 °C. Anal. ( $\text{C}_{48}\text{H}_{74}\text{N}_4\text{O}_{18}$ ) C, H, N.

**Compound 5.** Eluting solvent,  $\text{MeOH}/\text{CH}_2\text{Cl}_2/\text{EtOAc}/\text{toluene}/\text{aqueous } 28\% \text{ ammonia}$  (5:1:3:1:0.025); colorless oil; 85% yield;  $^1\text{H}$  NMR ( $\text{CDCl}_3$ , free base)  $\delta$  1.20–1.62 (m, 32H+2H exchangeable with  $\text{D}_2\text{O}$ ), 1.83 (t, 4H,  $J = 5.8$  Hz), 2.26 (t, 4H,  $J = 8$  Hz), 2.57 (t, 4H,  $J = 7$  Hz), 2.88 (d, 4H,  $J = 10.6$  Hz), 3.76 (s, 4H), 3.81 (s, 6H), 6.86–6.89 (m, 4H), 7.19–7.21 (m, 4H); EI-MS  $m/z$  650 ( $\text{M}^+$ ); mp (tetraoxalate salt) 182–184 °C. Anal. ( $\text{C}_{49}\text{H}_{76}\text{N}_4\text{O}_{18} \cdot 3\text{H}_2\text{O}$ ) C, H, N.

**Compound 6.** Eluting solvent, from  $\text{CHCl}_3/\text{EtOAc}/\text{MeOH}/\text{petroleum ether}/\text{aqueous } 28\% \text{ ammonia}$  (4:3:1.5:1:0.025) to  $\text{CH}_2\text{Cl}_2/\text{EtOAc}/\text{MeOH}/\text{toluene}/\text{aqueous } 28\% \text{ ammonia}$  (4:3:2:1:0.04); 58% yield;  $^1\text{H}$  NMR ( $\text{CDCl}_3$ , free base)  $\delta$  1.40–1.70 (m, 16H), 2.68 (t, 4H,  $J = 5$  Hz), 3.17 (t, 4H,  $J = 4.8$  Hz), 3.87 (s, 4H), 3.88 (s, 6H), 4.25 (br s, 4H exchangeable with  $\text{D}_2\text{O}$ ), 6.68–7.45 (m, 16H); EI-MS  $m/z$  624 ( $\text{M}^+$ ); mp (dioxalate salt) 223–224 °C. Anal. ( $\text{C}_{44}\text{H}_{58}\text{N}_4\text{O}_{10}$ ) C, H, N.

**Compound 7.** Eluting solvent,  $\text{MeOH}/\text{CHCl}_3/\text{toluene}/\text{aqueous } 28\% \text{ ammonia}$  (2:5:3:0.03), yellow pale oil; 54% yield;  $^1\text{H}$  NMR ( $\text{CDCl}_3$ , free base)  $\delta$  1.41–1.60 (m, 16H), 2.64 (t, 4H,  $J = 7$  Hz), 3.10 (t, 4H,  $J = 6$  Hz), 3.81 (s, 2H), 3.84 (s, 4H), 3.86 (s, 6H), 4.21 (br s, 4H exchangeable with  $\text{D}_2\text{O}$ ), 6.54–7.28 (m, 16H); EI-MS  $m/z$  637 ( $\text{M}^+$ ); mp (dioxalate salt) 168–169 °C. Anal. ( $\text{C}_{45}\text{H}_{60}\text{N}_4\text{O}_{10} \cdot 2\text{H}_2\text{O}$ ) C, H, N.

**Compound 8.** Eluting solvent,  $\text{MeOH}/\text{toluene}/\text{EtOAc}/\text{aqueous } 28\% \text{ ammonia}$  (1:4:5:0.04); yellow pale oil; 40% yield;  $^1\text{H}$  NMR ( $\text{CDCl}_3$ , free base)  $\delta$  1.44–1.62 (m, 16H), 2.66 (t, 4H,  $J = 6.8$  Hz), 2.82 (s, 4H), 3.12 (t, 4H,  $J = 6.1$  Hz), 3.85 (s, 4H), 3.88 (s, 6H), 4.24 (br s, 4H exchangeable with  $\text{D}_2\text{O}$ ), 6.57–7.29 (m, 16H); EI-MS  $m/z$  651 ( $\text{M}^+$ ); mp (dioxalate salt) 231–232 °C. Anal. ( $\text{C}_{46}\text{H}_{62}\text{N}_4\text{O}_{10}$ ) C, H, N.

## 7. Biology

### 7.1. Functional antagonism at guinea-pig left atria

Male guinea pigs (200–300 g) were killed by cervical dislocation. The heart was rapidly removed, and left atria were separated out and set up under 1 g of tension

in 20 mL organ baths containing physiological salt solution (PSS) maintained at 30 °C and aerated with 5%  $\text{CO}_2$ –95%  $\text{O}_2$ .

The left atria were mounted in PSS of the following composition (mM): NaCl, 118; KCl, 4.7;  $\text{CaCl}_2$ , 2.52;  $\text{MgSO}_4 \cdot 7\text{H}_2\text{O}$ , 1.18;  $\text{KH}_2\text{PO}_4$ , 1.18;  $\text{NaHCO}_3$ , 23.8; glucose, 11.7. Tissues were stimulated through platinum electrodes by square-wave pulses (1 ms, 1 Hz, 5–10 V) (Tetra Stimulus, N. Zagnoni). Inotropic activity was recorded isometrically. Tissues were equilibrated for 2 h, and a cumulative concentration–response curve to APE was constructed. Concentration–response curves were constructed by cumulative addition of the reference agonist. The concentration of agonist in the organ bath was increased approximately threefold at each step, with each addition being made only after the response to the previous addition had attained a maximal level and remained steady. Following 30 min of washing, tissues were incubated with the antagonist for 1 h, and a new dose–response curve to the agonist was obtained. Contractions were recorded by means of a force displacement transducer connected to the MacLab system PowerLab/800. In addition, parallel experiments in which tissues did not receive any antagonist were run in order to check any variation in sensitivity.

To quantify antagonist potency,  $\text{pK}_b$  values were calculated from the equation  $\text{pK}_b = \log(\text{DR}-1) - \log[\text{B}]$ , where DR is the ratio of  $\text{EC}_{50}$  values of agonist after and before treatment with 10  $\mu\text{M}$  concentration of the antagonist [B].<sup>53</sup>

### 7.2. Guinea pig ileum longitudinal muscle

The terminal portion of the ileum was excised after discarding the 8–10 cm nearest to the ileo-cecal junction. The tissue was cleaned, and segments 2–3 cm long of ileum longitudinal muscle were set up under 1-g tension at 37 °C in organ baths containing PSS of the following composition (mM): NaCl, 118; KCl, 4.75;  $\text{CaCl}_2$ , 2.54;  $\text{MgSO}_4$ , 1.2;  $\text{KH}_2\text{PO}_4 \cdot 2\text{H}_2\text{O}$ , 1.19;  $\text{NaHCO}_3$ , 25; glucose, 11. Tension changes were recorded isotonicity. Tissues were allowed to equilibrate for at least 30 min during which time the bathing solution was changed every 10 min. Concentration–response curves to APE (0.01–0.5  $\mu\text{M}$ ) were obtained at 30-min intervals, the first one being discarded and the second one taken as control. Following incubation with the antagonist for 60 min, a new concentration–response curve to the agonist was obtained.

### 7.3. Rabbit stimulated vas deferens

This preparation was set up according to Eltze.<sup>54</sup> Vas deferens were carefully dissected free of surrounding tissue and was divided into four segments, two prostatic portions of 1 cm and two epididymal portions of approximately 1.5 cm length. The four segments were mounted in PSS with the following composition (mM): NaCl 118.4, KCl (4.7),  $\text{CaCl}_2$  (2.52),  $\text{MgCl}_2$  (0.6),  $\text{KH}_2\text{PO}_4$  (1.18),  $\text{NaHCO}_3$  (25), glucose (11.1);  $10^{-6}$  M

yohimbine was included to block  $\alpha_2$ -adrenoceptors. The solution was maintained at 30 °C and tissues were stimulated through platinum electrodes by square-wave pulses (0.1 ms, 2 Hz, 10–15 V). Contractions were measured isometrically after tissues were equilibrated for 1 h, then a cumulative dose–response curve to pCl-McN-A-343 was constructed.

#### 7.4. Determination of antagonist potency

To quantify antagonist potency,  $pK_b$  values were calculated from the equation  $pK_b = \log(DR-1) - \log[B]$ , where DR is the ratio of  $ED_{50}$  values of agonist after and before treatment with one or two antagonist concentrations [B].<sup>55</sup>

#### 7.5. Inhibition of AChE and BChE

The method of Ellman et al. was followed.<sup>56</sup> Five different concentrations of each compound were used in order to obtain inhibition of AChE or BChE activity comprised between 20% and 80%. The assay solution consisted of a 0.1 M phosphate buffer, pH 8.0, with the addition of 340  $\mu$ M 5,5'-dithio-bis(2-nitrobenzoic acid), 0.035 U/mL of human recombinant AChE or BChE derived from human erythrocytes and serum, respectively (0.39 and 5.9 UI/mg, respectively; Sigma Chemical), and 550  $\mu$ M of substrate (acetylthiocholine iodide or butyrylthiocholine iodide). Test compounds were added to the assay solution and preincubated with the enzyme at 37 °C for 20 min followed by the addition of substrate. Assays were performed with a blank containing all components except AChE or BChE in order to account for non-enzymatic reaction. The reaction rates were compared and the percent inhibition due to the presence of test compounds was calculated. Each concentration was analyzed in triplicate, and  $IC_{50}$  values were determined graphically from log concentration–inhibition curves.

#### 7.6. Determination of ACh release by cerebral microdialysis

Microdialysis was performed in rat parietal cortex as described by Giovannini et al.<sup>50</sup>

The coordinates used for the implantation of the horizontal microdialysis tubing (AN 69 membrane, molecular weight cut off <15 kDa; Dasco, Italy) were AP 0.5 mm and H 2.3 mm from the bregma.<sup>57</sup> One day after surgery, the microdialyzing tubing was perfused at a constant flow rate (2  $\mu$ L/min) with Ringer's solution (NaCl 147, KCl 4.0,  $CaCl_2$  1.2 mM) containing 7  $\mu$ M physostigmine sulfate. After a 1-h settling period, the perfusate was collected at 20 min intervals in test tubes containing 5  $\mu$ L of 0.5 mM HCl to prevent ACh hydrolysis. The samples were then assayed for ACh content either immediately or after freezing. ACh was detected and quantified by HPLC with an electrochemical detector as described by Damsma et al.<sup>58</sup> ACh release was expressed as a percentage change over the mean of the first three basal samples as controls.

### 8. Binding experiments

#### 8.1. Cell culture and membrane preparation

CHO cells, stably expressing the human muscarinic ( $M_1$ – $M_5$ ) receptors (provided by Prof. R. Maggio, Department of Neuroscience, University of Pisa, Italy), were grown in Dulbecco's modified Eagle's medium, supplemented with 10% foetal bovine serum (Gibco, Grand Island, NY), 100 U/mL of penicillin G and streptomycin, 4 mM glutamine (Sigma Aldrich, Milano, Italy) and nonessential aminoacid solution  $100\times$  (Sigma Aldrich, Milano, Italy), and 50  $\mu$ g/mL of geneticin (Gibco, Grand Island, NY) in a humidified atmosphere consisting of 5%  $CO_2$  and 95% air. Confluent CHO cell lines were harvested by trypsinization, followed by centrifugation (300g for 5 min), washed with buffer (25 mM sodium phosphate, containing 5 mM  $MgCl_2$  at pH 7.4), and homogenized for 30 s using an Ultra-Turrax (setting 5). The pellet was sedimented at  $17,000\times g$  for 15 min at 4 °C and the membranes were resuspended in the same buffer, rehomogenized with Ultra-Turrax, and stored at –80 °C.<sup>59</sup> An aliquot was taken for the assessment of protein content,<sup>60</sup> using the Bio-Rad protein assay reagent (Bio-Rad Laboratories, München, West Germany). BSA was used as the standard.

#### 8.2. Binding assay

The radioligand binding assay was run in polypropylene 96-well plates (Sarstedt, Verona, Italy) and performed for 120 min at room temperature in a final volume of 0.25 mL in 25 mM sodium phosphate buffer containing 5 mM  $MgCl_2$  at pH 7.4. Final membrane protein concentrations were 30  $\mu$ g/mL ( $M_1$ ), 70  $\mu$ g/mL ( $M_2$ ), 25  $\mu$ g/mL ( $M_3$ ), 50  $\mu$ g/mL ( $M_4$ ), and 25  $\mu$ g/mL ( $M_5$ ). In homologous competition curves, [ $^3H$ ] N-methylscopolamine chloride, [ $^3H$ ] NMS, was present at 0.2 nM in tubes containing increasing concentrations of unlabeled NMS (0.03–1000 nM) and at 0.075–0.2 nM in tubes without unlabeled ligand. In heterologous competition curves, fixed concentrations of the tracer (0.2 nM) were displaced by increasing concentrations of several unlabeled ligands (0.01–1000  $\mu$ M). All measurements were obtained in duplicate. After incubation, membranes were filtered through UniFilter GF/C plates (Perkin-Elmer Life and Analytical Science, Boston, MA) using a FilterMate Cell Harvester (Perkin Elmer Life and Analytical Science, Boston, MA); filters were washed several times with ice-cold buffer and allowed to dry overnight at room temperature under air flow, 25  $\mu$ L of scintillation liquid (Microscint-20, Perkin Elmer Life and Analytical Science, Boston, MA) was added. Counting was done with TopCount NXT Microplate Scintillation Counter (Perkin Elmer Life and Analytical Science, Boston, MA).

#### 8.3. Statistical analysis

Data were analyzed using a pharmacological computer program.<sup>61</sup> Values are given as means  $\pm$  standard error of  $n$  independent observations. Student's  $t$  test was used to assess the statistical significance of the difference



between two means. The binding data were evaluated quantitatively with the weighted least-squares iterative curve fitting LIGAND program<sup>62</sup>; this analysis provides optimal estimates of binding parameters for the labeled ligand from the analysis of homologous curves: affinity constant ( $K_D$ ), binding capacities ( $B_{\max}$ ), and nonspecific binding ( $N$ ). Moreover, data from heterologous and homologous competition curves were simultaneously analyzed to obtain the  $K_i$  values for the unlabeled ligands. All the quoted values are means  $\pm$  SEM.

### Acknowledgment

This research was supported by grants from MIUR, Rome (FIRB RBNE03FH5Y and PRIN funds).

### Supplementary data

Supplementary data associated with this article can be found, in the online version, at [doi:10.1016/j.bmc.2007.01.022](https://doi.org/10.1016/j.bmc.2007.01.022).

### References and notes

- Caulfield, M. P. *Pharmacol. Ther.* **1993**, *58*, 319–379.
- Eglen, R. M. *Prog. Med. Chem.* **2005**, *43*, 105–136.
- Caulfield, M. P.; Birdsall, N. J. *Pharmacol. Rev.* **1998**, *50*, 279–290.
- Wang, H.; Lu, Y.; Chen, H. *Shengli Kexue Jinzhan* **2003**, *34*, 156–158.
- Yamada, M.; Basile, A. S.; Fedorova, I.; Zhang, W.; Duttaroy, A.; Cui, Y.; Lamping, K. G.; Faraci, F. M.; Deng, C. X.; Wess, J. *Life Sci.* **2003**, *74*, 345–353.
- Eglen, R. M.; Nahorski, S. R. *Br. J. Pharmacol.* **2000**, *130*, 13–21.
- Hulme, E. C.; Lu, Z. L.; Saldanha, J. W.; Bee, M. S. *Biochem. Soc. Trans.* **2003**, *31*, 29–34.
- Felder, C. C.; Bymaster, F. P.; Ward, J.; DeLapp, N. *J. Med. Chem.* **2000**, *43*, 4333–4353.
- Zlotos, D. P.; Bender, W.; Holzgrabe, U. *Expert Opin. Ther. Pat.* **1999**, *9*, 1029–1053.
- Wess, J. *Trends Pharmacol. Sci.* **2003**, *24*, 414–420.
- Matsui, M.; Yamada, S.; Oki, T.; Manabe, T.; Taketo, M. M.; Ehlert, F. J. *Life Sci.* **2004**, *75*, 2971–2981.
- Wess, J.; Zhang, W.; Duttaroy, A.; Miyakawa, T.; Gomez, J.; Cui, Y.; Basile, A. S.; Bymaster, F. P.; McKinzie, D. L.; Felder, C. C.; Deng, C.; Yamada, M. *Handbook of Experimental Pharmacology* **2004**, *159*, 65–93.
- Gawade, S. P. *J. Toxicol., Toxin Rev.* **2004**, *23*, 37–96.
- Bradley, K. N. *Pharmacol. Ther.* **2000**, *85*, 87–109.
- Potter, L. T. *Life Sci.* **2001**, *68*, 2541–2547.
- Potter, L. T.; Flynn, D. D.; Liang, J. S.; McCollum, M. H. *Prog. Brain Res.* **2004**, *145*, 121–128.
- Hulme, E. C.; Lu, Z. L.; Bee, M.; Curtis, C. A.; Saldanha, J. *Life Sci.* **2001**, *68*, 2495–2500.
- Shi, L.; Javitch, J. A. *Annu. Rev. Pharmacol. Toxicol.* **2002**, *42*, 437–467.
- Eglen, R. M.; Choppin, A.; Watson, N. *Trends Pharmacol. Sci.* **2001**, *22*, 409–414.
- Abrams, P.; Andersson, K. E.; Buccafusco, J. J.; Chapple, C.; de Groat, W. C.; Fryer, A. D.; Kay, G.; Laties, A.; Nathanson, N. M.; Pasricha, P. J.; Wein, A. J. *Br. J. Pharmacol.* **2006**, *148*, 565–578.
- Hegde, S. S. *Br. J. Pharmacol.* **2006**, *147*, S80–S87.
- Celli, B. R. *Ther. Strateg. COPD* **2005**, 93–105.
- Sheardown, M. J. *Expert Opin. Ther. Pat.* **2002**, *12*, 863–870.
- Clader, J. W.; Wang, Y. *Curr. Pharm. Des.* **2005**, *11*, 3353–3361.
- Messer, W. S., Jr. *Cogn. Enhancing Drugs* **2004**, 37–48.
- Koch, H. J.; Haas, S.; Jurgens, T. *Curr. Med. Chem.* **2005**, *12*, 2915–2921.
- Bartolini, A.; Ghelardini, C.; Fantetti, L.; Malcangio, M.; Malmberg-Aiello, P.; Giotti, A. *Br. J. Pharmacol.* **1992**, *105*, 77–82.
- Ghelardini, C.; Galeotti, N.; Bartolini, A. *Br. J. Pharmacol.* **2000**, *129*, 1633–1640.
- Wess, J.; Duttaroy, A.; Gomez, J.; Zhang, W.; Yamada, M.; Felder, C. C.; Bernardini, N.; Reeh, P. W. *Life Sci.* **2003**, *72*, 2047–2054.
- Bartolini, A.; Ghelardini, C.; Galeotti, N. *Recent Dev. Pain Res.* **2005**, 289–312.
- Melchiorre, C.; Angeli, P.; Brasili, L.; Giardina, D.; Gulini, U.; Pignini, M.; Quaglia, W. *Actualites Chim. Ther.* **1988**, *15*, 149–168.
- Bolognesi, M. L.; Minarini, A.; Budriesi, R.; Cacciaguerra, S.; Chiarini, A.; Spampinato, S.; Tumiatti, V.; Melchiorre, C. *J. Med. Chem.* **1998**, *41*, 4150–4160.
- Melchiorre, C.; Antonello, A.; Banzi, R.; Bolognesi, M. L.; Minarini, A.; Rosini, M.; Tumiatti, V. *Med. Res. Rev.* **2003**, *23*, 200–233.
- Melchiorre, C.; Cassinelli, A.; Quaglia, W. *J. Med. Chem.* **1987**, *30*, 201–204.
- Melchiorre, C. *Med. Res. Rev.* **1990**, *10*, 327–349.
- Tumiatti, V.; Andrisano, V.; Banzi, R.; Bartolini, M.; Minarini, A.; Rosini, M.; Melchiorre, C. *J. Med. Chem.* **2004**, *47*, 6490–6498.
- Tumiatti, V.; Rosini, M.; Bartolini, M.; Cavalli, A.; Marucci, G.; Andrisano, V.; Angeli, P.; Banzi, R.; Minarini, A.; Recanatini, M.; Melchiorre, C. *J. Med. Chem.* **2003**, *46*, 954–966.
- Melchiorre, C.; Andrisano, V.; Bolognesi, M. L.; Budriesi, R.; Cavalli, A.; Cavarini, V.; Rosini, M.; Tumiatti, V.; Recanatini, M. *J. Med. Chem.* **1998**, *41*, 4186–4189.
- Melchiorre, C.; Bolognesi, M. L.; Budriesi, R.; Ghelardini, C.; Chiarini, A.; Minarini, A.; Rosini, M.; Tumiatti, V.; Wade, E. J. *J. Med. Chem.* **2001**, *44*, 4035–4038.
- Marucci, G.; Novi, F.; Banzi, R.; Bolognesi, M. L.; Buccioni, M.; Minarini, A.; Rosini, M.; Angeli, P.; Maggio, R.; Melchiorre, C. *Med. Chem. Res.* **2004**, *13*, 63–73.
- Rosini, M.; Bixel, M. G.; Marucci, G.; Budriesi, R.; Krauss, M.; Bolognesi, M. L.; Minarini, A.; Tumiatti, V.; Hucho, F.; Melchiorre, C. *J. Med. Chem.* **2002**, *45*, 1860–1878.
- Budriesi, R.; Cacciaguerra, S.; Toro, R. D.; Bolognesi, M. L.; Chiarini, A.; Minarini, A.; Rosini, M.; Spampinato, S.; Tumiatti, V.; Melchiorre, C. *Br. J. Pharmacol.* **2001**, *132*, 1009–1016.
- Tumiatti, V.; Andrisano, V.; Banzi, R.; Bartolini, M.; Minarini, A.; Rosini, M.; Melchiorre, C. *J. Med. Chem.* **2004**, *47*, 6490–6498.
- Kenakin, T. P.; Boselli, C. *Naunyn Schmiedeberg's Arch. Pharmacol.* **1991**, *344*, 201–205.
- Ringdahl, B. *Mol. Pharmacol.* **1987**, *31*, 351–356.
- Eltze, M. *Eur. J. Pharmacol.* **1988**, *151*, 205–221.
- Van Rossum, J. M. *Arch. Int. Pharmacodyn. Ther.* **1963**, *143*, 299–330.
- Eltze, M.; Figala, V. *Eur. J. Pharmacol.* **1988**, *158*, 11–19.
- O'Callaghan, J. P.; Holtzman, S. G. *J. Pharmacol. Exp. Ther.* **1975**, *192*, 497–505.
- Giovannini, M. G.; Casamenti, F.; Nistri, A.; Paoli, F.; Pepeu, G. *Br. J. Pharmacol.* **1991**, *102*, 363–368.

51. Ellman, G. L.; Courtney, K. D.; Andres, V., Jr.; Featherstone, R. M.. *Biochem. Pharmacol.* **1961**, 7, 88–95.
52. Tumiatti, V.; Rosini, M.; Bartolini, M.; Cavalli, A.; Marucci, G.; Andrisano, V.; Angeli, P.; Banzi, R.; Minarini, A.; Recanatini, M.; Melchiorre, C. *J. Med. Chem.* **2003**, 46, 954–966.
53. Van Rossum, J. M. *Arch. Int. Pharmacodyn. Ther.* **1963**, 143, 299–330.
54. Eltze, M. *Pharmacology* **1988**, 37(Suppl. 1), 40–47.
55. Van Rossum, J. M. *Arch. Int. Pharmacodyn. Ther.* **1963**, 143, 299–330.
56. Ellman, G. L.; Courtney, K. D.; Andres, V.; Featherstone, R. M. *Biochem. Pharmacol.* **1961**, 7, 88–95.
57. Paxinos, W. G. *The rat brain in stereo-taxic coordinates*; Academic Press: New York, 1982.
58. Damsma, G. L. V. B. D.; Westerink, B. H. C.; Horn, A. S. *Chromatographia* **1987**, 24, 827–831.
59. Dei, S.; Angeli, P.; Bellucci, C.; Buccioni, M.; Gualtieri, F.; Marucci, G.; Manetti, D.; Matucci, R.; Romanelli, M. N.; Scapecchi, S.; Teodori, E. *Biochem. Pharmacol.* **2005**, 69, 1637–1645.
60. Bradford, M. M. *Anal. Biochem.* **1976**, 72, 248–254.
61. Motulsky, H. J. *Analyzing Data with GraphPad Prism*; GraphPad Software Inc.: San Diego, CA, 1999.
62. Munson, P. J.; Rodbard, D. *Anal. Biochem.* **1980**, 107, 220–239.